Energy, Mines and Resources Canada | Énergie, Mines et Ressources Canada

CANMET

Canada Centre for Mineral and Energy Technology | Centre canadien de la technologie des minéraux et de l'énergie

CATALYSTS SUPPORTED ON HYDROUS TITANATES FOR HYDROPROCESSING MIXTURES OF HEAVY OIL AND COAL

J. Monnier, G. Dénès, J. Potter and J.F. Kriz

AUGUST 1986

ENERGY RESEARCH PROGRAM
ENERGY RESEARCH LABORATORIES
DIVISION REPORT ERP/ERL 86-48 (J)

CATALYSTS SUPPORTED ON HYDROUS TITANATES FOR HYDROPROCESSING MIXTURES OF HEAVY OIL AND COAL

J. Monnier, G. Dénès[a], J. Potter[b] and J.F. Kriz

CANMET Energy Research Laboratories
Energy, Mines and Resources Canada
Ottawa, K1A 0G1 CANADA

ABSTRACT

Hydroprocessing catalysts were prepared by ion exchange of a sodium hydrous titanate support with aqueous solutions of transition metals (Ni, Co, Mo, Zn) or main group elements (Sn, Al). These catalysts were tested in an autoclave system with a constant flow of hydrogen for the hydrocracking of mixtures of one part subbituminous coal and two parts residual oil from vacuum distillation of an Alberta heavy oil. The operating pressure and temperature were chosen so that the hydrocracking reactions occurred at the threshold of coking. Catalysts were compared on the basis of yields of oil, asphaltenes and

---

[a] Department of Chemistry and Laboratories for Inorganic Materials, Concordia University, Montréal, Qué., H3G 1M8

[b] Energy Research Unit, University of Regina, Regina, Sask., S4S 0A2

preasphaltenes, conversion of THF-insolubles, and sulphur content in the hydrocarbon distillates collected from exiting gases. The presence of semicoke was determined by petrographic analysis of samples of THF-insolubles. Mössbauer spectroscopy provided information on the chemical changes occurring to the tin active sites during reaction, and X-ray powder diffraction, on the nature of the crystalline phases present in these catalysts and on their average particle dimension. Experimental results indicate that some metal-exchanged hydrous titanates can help produce more pentane-soluble oil and less gas than commercial hydrotreating catalysts.

INTRODUCTION

In recent years, coal conversion research and development has focused on the concept of coprocessing where coal is hydrogenated in the presence of bitumen or heavy oil of petroleum origin (Monnier, 1984; Kelly et al., 1985; Ignasiak et al., 1985; McLean and Duddy, 1986; C&EN, 1986). Coprocessing is an attractive alternative in Canada where large deposits of both coal and heavy oil are found in geographical proximity. An economic advantage over conventional liquefaction may be in the elimination of recycle streams of coal-derived liquids. However the principal advantage in coprocessing is the increase in distillate yield based on the amount of heavy oil used. As in any process utilizing high-pressure hydrogen, better conversions and liquid product quality can be achieved by the addition of catalysts to the feed slurry (Curtis et al., 1985; Monnier and Kriz,

1985). Recently, the Sandia National Laboratories of the U.S. Department of Energy developed new catalyst supports for coal hydrogenation utilizing metal-exchanged hydrous titanates (Dosch et al., 1985; Stephens et al., 1985). In our laboratory catalysts prepared in a similar manner were applied in the coprocessing of residual oil and coal. The present study discusses the results obtained.

EXPERIMENTAL

Catalyst preparation

Metal-exchanged hydrous titanates (MEHT) were prepared according to the method of Dosch, Stephens and co-workers (1985). The catalyst support is produced by reacting titanium(IV) isopropoxide, $Ti[OCH(CH_3)_2]_4$, with a solution of sodium hydroxide in methanol to produce a soluble intermediate, and precipitating the sodium hydrous titanate, $NaTi_2O_5H$, using a mixture of 10 wt % water in acetone. The precipitate is washed with water and acetone, then dried under vacuum. The resulting material is a white, fluffy powder which can be loaded with a metal from an aqueous solution of its salt via the exchange with the sodium ions. The catalyst is then washed with water and acetone, and dried under vacuum overnight. Before being tested for hydroprocessing, the titanate catalysts are calcined in air at 400°C for 2 hours. Cobalt-molybdenum supported on alumina (Harshaw HT-400E) was used in a powder form (grain size <149 μm) as the reference

catalyst.

The composition of the calcined MEHT catalysts, analyzed by inductively coupled argon plasma spectrometry and neutron activation, is presented in Table 1. Their surface area, measured by (BET) nitrogen adsorption, varied from 60 to 150 m^2/g. Pore volume data were obtained by mercury porosimetry using a Micromeritics Autopore 9200. Information on the size and shape of the catalyst particles, at various stages of their preparation, was provided by scanning electron microscopy, using a Hitachi S-520 scanning electron microscope operating with the filament energized at 15 kV. The catalysts for electron microscopy were dried at 120°C overnight to remove adsorbed water, then stored in a dessicator and gold-coated.

Mössbauer spectroscopy and X-ray diffraction of the tin-containing catalysts

Information on the oxidation state and chemical environment of the metal active sites in some catalysts can be provided by Mössbauer spectroscopy. Since among the metals used in this work only tin has a convenient Mössbauer isotope, samples of tin catalysts were analyzed by ^{119}Sn Mössbauer spectroscopy (MS). The 23.875 keV Mössbauer γ-ray line was obtained using a 15 mCi $Ca^{119m}SnO_3$ source purchased from Amersham with a 0.1-mm thick Pd foil filter. All spectra were recorded with both the source and absorber (sample) at ambient temperature. The amount of sample used was determined in order to have 10 mg Sn/cm^2. The spectra were calibrated using α-SnF_2 and

$CaSnO_3$ as standards. Computer fitting was performed using GMFP5 (Monnier et al.,1984), a revised version of the General Mössbauer Fitting Program (GMFP) of Ruebenbauer and Birchall (1979). All chemical isomer shifts are given relative to $CaSnO_3$ at room temperature [$\delta(CaSnO_3) = 0$ at RT].

X-ray powder diffraction tests, performed on the same tin samples to complement the Mössbauer data (X-ray diffraction giving long range order, Mössbauer spectroscopy being a local probe) were expected to reveal information on the structure of the catalysts. All X-ray powder patterns were recorded using the Cu K-alpha radiation ($\lambda_{K\alpha Cu}$ = 1.54178 Å), using a Ni foil filter.

Catalytic hydroprocessing tests

The hydrocarbon feedstock was a mixture of 33 wt % Forestburg subbituminous C coal (as received) and 67 wt % Cold Lake vacuum bottoms (CLVB) from an Alberta heavy oil reservoir. As shown in Table 2, CLVB is about 72 wt % oil (pentane soluble) and contains about 5.5 wt % sulphur. Table 2 also gives the proximate and ultimate analyses of the coal used as fine particles smaller than 149 μm diameter. To simplify handling, 60 g of coal and heavy oil was placed inside a reactor liner with 3.2 g of catalyst.

Initially, the feed slurry of coal and residual oil contained about 2.3 wt % sulphur which, depending on the catalyst, corresponded to a minimum of 12 atoms S per atom of exchanged cation.

It was thus expected that sulphiding would occur in situ under reaction conditions by contact with the liquid phase rich in sulphur compounds (Ternan and Whalley, 1976). Consequently, no presulphiding procedures were applied in any case. It should also be mentioned that in a continuous reactor system, a "disposable" catalyst would probably be added without any pretreatment to the slurried feed and then discarded after primary upgrading of the heavy oil-coal mixture.

The catalytic hydroprocessing tests were performed at 410°C in a 300-mL stirred autoclave equipped to operate under continuous hydrogen flow. A back-pressure regulator maintained the pressure inside the autoclave at 3.4 MPa. A cold trap placed before this regulator removed the distillates from the outlet gases. The hydrogen flowrate of about 275 mL (STP)/min was sufficient to replace the internal gas volume in about 15 min. The system temperature and pressure conditions were chosen so that reaction occurred at the threshold of coking as shown previously (Monnier and Kriz, 1985). A reaction time of 225 min was maintained in an attempt to observe the hydroprocessing selectivity while reasonably enhancing the distillate yield.

On completion of a run, the oil remaining in the autoclave (between the wall and the reactor liner) was drained. The distillates were the liquids including aqueous portions collected from the trap. Tetrahydrofuran (THF) used to remove residues from the metal liner was subsequently evaporated in a vacuum oven.

The residues were analyzed by solvent extraction for the oil content (pentane solubles), asphaltenes (pentane insolubles - toluene solubles), preasphaltenes (toluene insolubles - THF solubles) and THF insolubles. Total oil yield was calculated by adding the weight of the distillates excluding water and the oil drained from the autoclave to the weight of pentane solubles. The distillates were characterized by elemental analysis and by gas chromatography - simulated distillation. The outlet gases were analyzed by gas chromatography.

Semicoke formation was determined by petrographic analysis of samples of THF-insolubles. This analysis was carried out in plane-polarized light, on the polished, pelleted samples using a Leitz "Orthoplan-pol" incident light microscope, at a magnification of 500 x. An accessory λ plate was inserted in the light path to enhance the optical properties of anisotropic solids and facilitate the identification of anisotropic semicokes. The relative abundances (volume per cent) of unaltered coal, altered coal, granular residue, coal/pitch-derived solids and mineral matter, terms which are defined in the Discussion section, were measured by point counting with the aid of a Swift automatic point counter and a Leitz "click-stop" sample holder.

CATALYST CHARACTERIZATION

Scanning electron microscopy

Figures 1 and 2 present SEM micrographs of MEHT catalysts at two stages of their preparation. In the first figure, the sodium hydrous titanate support is shown after overnight drying under vacuum at room temperature. It consists of 1-2 μm diam. particles having an irregular shape and probably composed of smaller grains since no Bragg peak was observed by X-ray diffraction. After cationic exchange and catalyst calcination, these 1-μm particles agglomerate to give very porous lumps of materials varying in size from 30 to 60 μm (Fig. 2). Calcination of the support without any exchange also leads to agglomeration.

Mercury porosimetry

The expected high porosity of these catalysts was confirmed by mercury porosimetry. In Fig. 3, the pore distribution of a cobalt-molybdenum hydrous titanate (MB-592), which is plotted as an incremental pore volume versus pore diameter, is compared with that of a commercial alumina-supported catalyst containing the same metals (MB-531). A very wide range of pore diameters is observed for MB-592, with a minimum size of about 150 Å. Such a distribution of pore diameters can be advantageous in facilitating the diffusion, to the metal active sites, of large "molecules" of asphaltenes and preasphaltenes, the size of which range in the hundreds of angstroms

(Baltus, 1984). This contrasts remarkably with the narrow pore distribution of MB-531 which is centered at about 90 Å.

X-ray powder diffraction

a. Phase identification

Figures 4 and 5 present results of X-ray powder diffraction for two tin catalysts, MB-586 and MB-599 respectively, which were made with slightly different titanate supports: in the case of MB-599, the reaction of titanium(IV) isopropoxide with the solution of NaOH in CH_3OH was performed at a lower temperature than for the support of MB-586, in order to avoid formation of some cloudiness in the mixture containing the soluble intermediate.

None of the preparations of sodium hydrous titanate supports gives rise to Bragg peaks (Fig. 4a and 5a), showing that these samples are amorphous or microcrystalline (particle size <50 Å). The same was reported by Stephens et al. (1985) for supports prepared using a similar procedure.

The non-calcined tin catalysts (Fig. 4b and 5b), dried at room temperature under vacuum, are also poorly crystallized. However, careful examination reveals two very broad scattering rings barely distinguishable from the background and spread over several degrees theta, which are in part attributed to microcrystalline (40 to 50 Å diameter) TiO_2 and SnO_2.

Calcination of the tin catalysts results in significant growth of the particles as shown in the X-ray powder patterns (Fig. 4c and 5c) by the presence of several groups of overlapping Bragg peaks. However, these peaks are still considerably broadened, showing that the particle size, although larger, is still very small, such that the samples must still be classified as microcrystalline.

The main crystalline component of the calcined MB-586 catalyst (Fig. 4c) is clearly TiO_2 anatase (ASTM 4-0477). In addition, SnO_2 rutile (ASTM 5-0467) and TiO_2 rutile (ASTM 21-1276) in lower amounts are also observed. The calcined MB-599 catalyst (Fig. 5c) gives clusters of broad peaks at about the same theta values as calcined MB-586. However, it is clear that the structure of these clusters is quite different. In contrast to MB-586, no TiO_2 anatase is present. In addition, the top of each peak is located between the corresponding peaks of TiO_2 and SnO_2 rutiles ruling out their presence in MB-599 and indicating that a rutile-type $Ti_{1-x}Sn_xO_2$ solid solution had formed. Its cell parameters are intermediate between those of SnO_2 and TiO_2 rutile as shown below:

Unit cell parameters	TiO_2	$Ti_{1-x}Sn_xO_2$	SnO_2
a (Å)	4.594	4.643	4.738
c (Å)	2.958	3.100	3.188
V ($Å^3$)	62.43	66.83	71.51

The pattern of the solid solution was indexed in a rutile cell, assigning the two first peaks the indexation (110) and (101). The unidentified peak on calcined MB-586 (X in Fig. 4c) corresponds to the (101) peak of $Ti_{1-x}Sn_xO_2$ observed on calcined MB-599, indicating that a smaller amount of mixed tin-titanium oxide solid solution had also formed in calcined MB-586.

b. Particle dimension

The average particle size of the tin catalysts was determined using Scherrer formula (Cullity, 1978). All other causes of broadening, mainly instrumental, were accounted for with α-SnF_2 using Warren's method (Cullity, 1978). The results are given in Table 3. It is obvious these results are not very accurate because of the strong peak overlapping due to the multiphasic nature of the samples. However, it is clear that the samples are microcrystalline with an average particle diameter in the range 100 to 300 Å with the anatase particles being two to three times larger than the $Ti_{1-x}Sn_xO_2$ crystallites. This shows that the particles from 30 to 60 μm observed in electron microscopy on calcined samples (Fig. 2) are, indeed, agglomerates of a large number (about 10^{10}) of much smaller size particles (diameter about 1000 times smaller), which explains the irregular shape and absence of internal structure of the aggregates.

Mössbauer spectroscopy

Mössbauer spectroscopy, by probing shifts and splittings of the nuclear ground and first excited states of ^{119}Sn, provides information on the causes of these effects, i.e., oxidation state, electronic structure, ligand changes and coordination of tin. The relevant Mössbauer results for MB-586 and MB-599 are summarized in Table 4.

The non-calcined tin catalysts MB-586 and MB-599 (dried at room temperature under vacuum) contain tin in mixed oxidation states. Tetravalent tin is the major component for both catalysts, however there is a large difference in their Sn(II)/[Sn(II)+Sn(IV)] ratio (5% for MB-586, and 25% for MB-599). In these catalysts, before calcination, tin(IV) is undoubtedly in a pseudooctahedral coordination of oxygen (O^{2-}, OH^- or H_2O) similar to SnO_2 (Baggio and Sonnino, 1970) or its hydrates $SnO_2.xH_2O$ as observed in tin-treated coals (Cook et al., 1985). The divalent tin Mössbauer parameters are characteristic of a low coordination tin(II) with an environment strongly distorted by the stereoactive lone pair of electrons on tin which gives rise to large quadrupole splittings ($\Delta > 1.50$ mm.s^{-1}) (Birchall et al., 1981). Coordinations such as distorted SnX_3E tetrahedra and SnX_4E trigonal bipyramids (X = F or O, E = lone pair) are commonly encountered (Dénès et al., 1979; Dénès et al., 1980). The divalent tin species in these catalysts could not be identified with any of the tin(II) oxides or hydroxides or their hydrates reported in the literature, such as SnO, $SnO.yH_2O$ or $Sn_5O_3(OH)_4$. As these

tin(II) species give no visible diffraction pattern, they are probably also microcrystalline. The fact that they are mixed with other phases (hydrated tin(IV) and titanium(IV) oxides) precludes further characterization. It is also noteworthy that, before calcination, the two catalysts differ not only by the amount of tin(II) but also by their Mössbauer parameters which indicates a different environment.

Calcination at 400°C for 2 h in air oxidizes all tin(II) to tetravalent tin. This was expected as divalent tin, although usually stable at room temperature in air when in the solid state, undergoes oxidation in oxidizing atmosphere when the temperature is raised. The tin(IV) species was identified as being SnO_2 by X-ray diffraction, in agreement with the Mössbauer data. There is no significant difference between the Mössbauer parameters of calcined MB-586 and MB-599. This is not surprising as one would expect the coordination of tin(IV) in a rutile solid solution $Ti_{1-x}Sn_xO_2$ to be almost identical to that found in SnO_2, hence giving indistinguishable Mössbauer parameters.

TEST RESULTS AND DISCUSSION

Coprocessing tests were performed with MEHT catalysts containing different metal cations. Product distributions corresponding to the metal contained within the support are depicted in Fig. 6. It shows the yields of oil (O), asphaltenes (A) and preasphaltenes (P) expressed in weight per cent (maf) of the feed mixture. Coal conversion was measured in terms of THF insolubles (T)

before and after each run (ratio of shaded areas). This determination was thus complicated by the formation of THF-insoluble semicoke, an undesirable competing reaction, occurrence of which indicates the upper limit of the usable temperature range.

Figure 6 shows that the addition of a catalyst to the feed slurry enhances the conversion of THF insolubles and the oil yield. In the absence of catalysts, more of the THF-insoluble material is found in the product than in the feed slurry, which suggests the occurrence of coking at these experimental conditions and is confirmed by petrographic analysis described later in this section. However, in the presence of catalysts, up to 65 wt % of the THF-insoluble material in the feed was converted and oil yields up to 65% were observed.

The catalyst modification through exchange of sodium for molybdenum and palladium led to conversions of about 65% and 59% respectively. These conversions appear to be significantly higher than those observed for nickel and cobalt (about 47%). However, not all MEHT catalysts worked as well. For tin, the outcome was not significantly different from that observed without catalyst: the negative values of conversion indicating significant semicoke formation. Zinc-exchanged hydrous titanates catalyst performed somewhat better in terms of oil yield and conversion. It is of interest to note that good activity of tin and zinc chlorides and oxides, as coal liquefaction catalysts, was reported in the literature (Weller, 1956; Mizumoto et al., 1985).

Similarly, net gains in oil fraction were obtained for all metal cations except tin and zinc. The oil yields varied from 48 wt % for cobalt to 65 wt % for molybdenum. This may appear as a small gain when compared to the initial content of about 47 wt % in the feed slurry. However, one must also consider the difference in quality of the resulting oil of which 30 to 40% boils below the initial boiling point for CLVB in the feed. The performance of palladium was likely impeded by the high sulphur content in the feed slurry (about 2.3 wt %) but was still comparable to that of the sulphur-tolerant molybdenum. For tin and zinc, the oil yields were from 36 to 40%, similar to the blank test. Performance variations between the individual metals could be caused by the differences in initial metal dispersions within the support or dispersion stabilities under reaction conditions.

To make a meaningful comparison between the hydrous titanates and the alumina-supported catalyst MB-531, a cobalt-molybdenum HT (MB-592) was prepared by successive cationic exchange in aqueous solutions of molybdenum and cobalt. Figure 7 presents the product distribution of both catalysts in coprocessing at 410 and 430°C. At both temperatures, MB-592 was superior in terms of oil yield by about 20%. As the temperature increases, the fraction of asphaltenes and preasphaltenes decreases for both catalysts, whereas the fraction of THF insolubles increases sharply.

As shown earlier, some of the MEHT catalysts produced up to 25% more oil than the reference catalyst (cobalt-molybdenum on alumina). Furthermore, the increase in oil yield with MEHT catalysts

was accompanied by a lower yield of gaseous hydrocarbons, such as methane, ethane and propane, as calculated by difference from the mass balance of the product distribution and shown in Fig. 8. Although a negative (gas + loss) value was observed, this was evidently caused by errors in the analysis. Six tests performed at identical reaction conditions with MB-531 gave an average gas yield of about 12 wt %. The MEHT catalysts, excluding tin and zinc, performed significantly better, the gas yield decreasing to an average value of about 5 wt %, based on 13 tests. Cracking reactions causing the formation of these hydrocarbons were evidently impeded, probably because of weaker surface acidity of these catalysts. With tin and zinc HT, the hydrogen transfer within the reacting hydrocarbon mixture was likely less effective, causing insufficient saturation of the large cracked intermediate molecules.

Figure 9 compares the MEHT catalysts with the reference catalyst MB-531 in terms of sulphur removal from the distillate oil collected in the trap (boiling range from 60 to 350°C). The sulphur concentrations are typically from 1.6 to 1.8 wt %, and thus are lower than the 1.9 wt % observed in the blank test. Multiple ion exchanges can provide MEHT catalysts containing more than one cation. Using a cobalt-molybdenum MEHT catalyst, the sulphur content is further lowered to 1.3 wt %, indicating that a better sulphur removal is achieved when Co-Mo type catalysts are used (Monnier and Kriz, 1985). Although the commercial cobalt-molybdenum supported on alumina still outperformed this MEHT catalyst in terms of sulphur removal, it was encouraging to note that the difference was less significant, leading to sulphur

levels in the product oil of 1.0 to 1.1 wt %. In the overall perspective, better refining can therefore be seen with the use of MB-592.

Petrographic analysis

Samples of THF-insoluble residues were characterized to determine the presence of anisotropic semicoke. Table 5 distinguishes 5 different solids found by petrographic anlysis. The coal/pitch-derived solids are intermediate product of coal/pitch conversion. Ultimately, they yield a granular residue as a by-product. This residue consists of a very fine-grained, carbonaceous material interdispersed with inorganic minerals. Similarly, the anisotropic semicoke can also be considered as a by-product (from coal or coal/pitch-derived solids), but from a different process involving mainly carbonization reactions that occur when the hydrogen transfer is insufficient within the reaction mixture for hydrogenation reactions to proceed (Belinko et al.,1979). The anisotropic semicoke is easily detected when the polars of the microscope are crossed or partially crossed. Altered coal is unconverted coal which has been thermally or chemically affected and finally, the fraction of unaltered coal represents reactive macerals which have not been affected by chemical or thermal treatment during coprocessing. Additional details can be found in the literature (Potter, 1986).

The results in Table 5 confirm the presence of anisotropic

semicoke in tests with negative conversion (corresponding to the blank test and the tests with Zn HT or Sn HT). However, some coal/pitch-derived intermediates were present but the absence of granular residues in these particular samples precludes any significant extent of liquefaction during these tests. With Mo, Ni, Co, Pd and Co-Mo hydrous titanates which produced high oil yields, the fraction of granular residue was appreciable, accounting for up to 16.1 vol % of the THF-insolubles. The absence of semicoke in these tests, even after the relatively long residence time, suggests that these catalysts provided effective hydrogen transfer during the full length of the tests.

X-ray diffraction characterization of the THF-insolubles

The THF-insoluble materials from the hydroprocessing tests with MB-586 and MB-599 were examined by X-ray diffraction. All diffraction patterns (Fig. 4d, 5d and 5e), corresponding to these catalyst-containing residues, seem to be similar and indicate the presence of TiO_2 anatase, TiO_2 rutile and SnO_2 rutile. Additional small new peaks visible in the pattern indicate the presence of SnS stannous sulphide (ASTM 14-620). Furthermore, the presence of a small quantity of elemental tin, ß-Sn (ASTM 4-0673), was a possibility. No tin(IV) sulphide or titanium(IV) sulphide was observed. Only the presence of sulphur (2.3 wt %) in the feed slurry of Cold Lake vacuum bottoms and Forestburg coal can explain the formation of tin(II) sulphide from tin(IV) oxide of the unused catalysts.

The used MB-599 catalyst was found to contain much more

TiO_2 anatase than the unused calcined catalyst. This alludes to formation of anatase during the hydroprocessing reaction. The change can be explained using the hypothesis of a $Ti_{1-x}Sn_xO_2$ solid solution in the calcined catalyst. Indeed, as no tin(II) is present in the calcined catalysts, simultaneous reduction and sulphidation of some of the tin in the solid solution must occur, which releases TiO_2 in the anatase polymorph. The following reactions can occur:

$$x\ S^{2-} + \underset{\text{rutile}}{Ti_{1-x}Sn_xO_2} + 2x\ H_2 \longrightarrow (1-x)\ \underset{\text{anatase}}{TiO_2} + 2x\ H_2O + SnS + 2\ e^-$$

$$x\ S^{2-} + \underset{\text{rutile}}{Ti_{1-x}Sn_xO_2} + 2x\ C \longrightarrow (1-x)\ \underset{\text{anatase}}{TiO_2} + 2x\ CO + SnS + 2\ e^-$$

Mössbauer spectroscopic characterization of the THF insolubles

The Mössbauer parameters of Table 5 indicate that, after coprocessing, part of the tin(IV) contained in the THF insolubles was reduced to SnS. This corroborates the X-ray results. Traces of ß-Sn suggested by diffraction could not be confirmed by Mössbauer spectroscopy because of the strong overlapping of the ß-Sn and SnS lines. However, in case ß-Sn is indeed formed, it can be present only in a small amount. The two tin catalysts tested were observed to form different amounts of SnS, MB-599 forming ten to fifteen times more SnS upon coprocessing. If this is attributed to the difference in composition, it would indicate that tin in $Ti_{1-x}Sn_xO_2$ is easier

to reduce than tin in SnO_2 under the reaction conditions, leading to more extensive formation of SnS and TiO_2 anatase upon coprocessing. Mössbauer spectroscopy also shows no evidence for the formation of mixed-oxidation state tin sulphides Sn_2S_3 or Sn_3S_4.

Calculations of equilibrium constants (Barin and Knacke, 1973) for the reduction of oxides of Sn, Mo, Co and Ni at reaction temperatures used in these experiments show that SnO_2 is more difficult to reduce in H_2 than NiO, CoO and MoO_3. Similar calculations indicate that the sulphides are relatively more stable than oxides of these metals. Thus, the presence of SnS in the THF insolubles suggests that formation of sulphides of the other metals occurs.

CONCLUSIONS

Metal-exchanged hydrous titanates have been investigated for the catalytic hydroprocessing of mixtures of coal and heavy oil. These MEHT catalysts consist of microcrystallites which agglomerate to give catalyst particles with large pores, facilitating the diffusion of heavy hydrocarbon molecules to the active sites. The performance of some MEHT catalysts (molybdenum, palladium, nickel, cobalt and cobalt-molybdenum) compared favourably with a commercial Co-Mo catalyst in terms of oil yield, conversion of THF insolubles and gas formation. The petrographic analysis of the THF-insoluble residues confirmed the conversion data obtained by solvent extraction. Mössbauer spectroscopy, corroborated by X-ray powder diffraction, showed that catalysts are

partially reduced and sulphided in the process. X-ray diffraction established the microcrystalline nature of the MEHT catalysts and allowed identification of the phases present and an estimation of their particle size. Electron microscopy showed the porosity of the samples and confirmed the small extent of crystallinity.

ACKNOWLEDGEMENTS

The authors wish to thank M.R. Fulton, P.Y. Dionne, P.S. Soutar, P. Zourdos, M. Skaff and J.-F. Bilodeau for technical assistance at CANMET; N. Kapoor and J. Fitzgerald, in the electron microscopic study, M. Dénès, in X-ray diffraction and W.G. McDougall, in the petrographic analysis. Financial assistance from Concordia University for the purchase of the Mössbauer spectrometer is acknowledged. G.D. thanks the Natural Science and Engineering Research Council of Canada for a University Research Fellowship.

REFERENCES

Baggio, E.M.; Sonnino, T.J., J. Chem. Phys. 1970, 52, 3786.

Baltus, R.E., in "Catalysis on the Energy Scene", Kaliaguine, S. and Mahay, A. Ed., Elsevier Science Publishers B.V., Amsterdam and New York, 553-560 (1984).

Barin, I.; Knacke. O., "Thermochemical properties of inorganic substances", Springer-Verlag, Berlin and New-York (1973).

Belinko, K.; Kriz, J.F.; Nandi, B.N., In preprints, 6th Canadian Symposium on Catalysis (1979).

Birchall, T.; Dénès, G.; Ruebenbauer, K.; Pannetier, J., J. Chem. Soc. (A), Dalton Tr. 1981, 1831-1836.

Chem. Eng. News 1986, 64(28), 26.

Cook, P.S.; Cashion, J.D.; Cassidy, P.J., Fuel 1985, 64, 1121-1126.

Cullity, B.D., " Elements of X-ray Diffraction", 2nd edition, Addison-Wesley Publishing Co., Inc., Don Mills, Ontario, pages 192 & 284 (1978).

Curtis, C.W.; Tsai, K.-J.; Guin, J.A., ACS Preprints, Div. of Petroleum Chemistry 1985, 30(4), 688-696.

Dénès, G.; Pannetier, J.; Lucas, J.; Le Marouille, J.Y., J. Solid State Chem. 1979, 30, 335-343.

Dénès, G.; Pannetier, J.; Lucas J., J. Solid State Chem. 1980, 33, 1-12.

Dosch, R.G.; Stephens, H.P.; Stohl, F.V., U.S. Patent 4 511 455, 1985.

Ignasiak, B.; Kovacik, G.; Ohuchi, T.; Lewkowicz, L.; du Plessis, M.P., in Proceedings Coal Conversion Contractors' Review Meeting, Calgary, November 1984, J.F. Kelly Ed., CANMET, Energy, Mines and Resources Canada, ISBN 0-660-53122-4, 385-395 (1985).

Kelly, J.F.; Fouda, S.A.; Rahimi, P.; Ikura, M., in Proceedings Coal Conversion Contractors' Review Meeting, Calgary, November 1984, J.F. Kelly Ed., CANMET, Energy, Mines and Resources Canada, ISBN 0-660-53122-4, 397-423 (1985).

McLean, J.B.; Duddy, J.E., ACS Preprints, Div. of Fuel Chemistry 1986, 31(4), 169-180.

Mizumoto, M.; Yamashita, H.; Matsuda, S., Ind. Eng. Chem. Prod. Res. Dev. 1985, 24(3) 394-397.

Monnier, J., CANMET Report 84-5E, CANMET, Energy, Mines and Resources Canada, ISBN 0-660-11683-9 (1984).

Monnier, J.; Dénès, G.; Anderson, R.B., Can. J. Chem. Eng. 1984, 62(3), 419-424.

Monnier, J.; Kriz, J.F., ACS Preprints, Div. of Petroleum Chemistry 1985, 30(3), 513-520.

Potter, J., "Characterization of solid residues from coal liquefaction processes", final report to CANMET under Supply and Services Canada contract No. 0ST85-00100, Energy Research Unit, University of Regina (1986).

Ruebenbauer, K.; Birchall, T., Hyperfine Interact. 1979, 7, 125-133.

Stephens, H.P.; Dosch, R.G.; Stohl, F.V., Ind. Eng. Chem. Prod. Res. Dev. 1985, 24(1), 15-20.

Ternan, M.; Whalley, M.J., Can. J. Chem. Eng. 1976, 54, 642-644.

Weller, S.W., in "Catalysis IV", P. Emmett Ed., Reinhold Publishing Company, Chapter 7 (1956).

Table 1: Composition of hydroprocessing catalysts

Catalyst	Composition (wt %)							
	Mo	Co	Pd	Sn	Zn	Ni	Na	Ti
MB-582	-	-	-	-	-	15.8	0.1	42.0
MB-586	-	-	-	12.7	-	-	1.1	43.2
MB-588	-	-	12.5	-	-	-	4.1	43.0
MB-592	10.1	5.0	-	-	-	-	0.1	40.5
MB-593	11.2	-	-	-	-	-	1.5	46.6
MB-596	-	-	-	-	11.4	-	5.6	47.5
MB-599	-	-	-	16.8	-	-	3.9	36.5
MB-602	-	7.8	-	-	-	-	6.0	41.2
MB-531(Ref.)	8.9	2.6	-	-	-	-	-	-

Table 2: Characteristics of feedstocks

Forestburg subbituminous C coal

Ultimate analysis (wt %)		Proximate analysis (wt %)	
Carbon	64.04	Moisture	9.2
Hydrogen	3.87	Ash	7.8
Sulphur	0.53	Volatiles	46.5
Nitrogen	1.65	Fixed carbon (by difference)	36.5
Oxygen	20.41		

Cold Lake vacuum bottoms

Ultimate analysis (wt %)		Other characteristics	
Carbon	84.04	IBP	420°C
Hydrogen	9.94	Oil	72.3%
Sulphur	5.46	Asphaltenes	27.7%
Nitrogen	0.63	-525°C	20%
Oxygen	0.50	+525°C	80%

Table 3: Average particle size of the tin catalysts as determined by Scherrer's method from the broadening of the Bragg peaks

Sample	Stage[a]	Θ[KαCu(°)]	B_M(°)[b]	B_S(°)[b]	B(°)[b]	t(Å)[b]	Compound
MB-586	c	12.70	0.32	0.17	0.27	301	TiO_2 anatase
MB-586	u	12.70	0.52	0.18	0.49	167	TiO_2 anatase
MB-599	c	13.58	0.70	0.17	0.68	120	$Ti_{1-x}Sn_xO_2$ rutile
MB-599	c	17.40	1.05	0.17	1.04	80	$Ti_{1-x}Sn_xO_2$ rutile
MB-599	u(63)	17.60	0.80	0.17	0.78	107	$Ti_{1-x}Sn_xO_2$ rutile
MB-599	u(76)	12.64	0.30	0.17	0.25	330	TiO_2 anatase
MB-599	u(76)	17.60	0.50	0.17	0.47	177	$Ti_{1-x}Sn_xO_2$ rutile

Notes:

a) Stage: c = calcined catalyst and u = used catalyst.
MB-599 was used in two reactions (run 63 refers to Fig. 9d and run 76 to Fig. 9e).

b) The average particle size t was obtained from Scherrer formula $t = (0.9\lambda)/(B.\cos\Theta)$, ($\lambda$ = wavelength, Θ = Bragg angle), corrected using Warren's method $B^2 = B_M^2 - B_S^2$ where B is the broadening at half height due to the small size of the particles, when B_M and B_S are the experimental values for the sample and for a well-crystalline standard, respectively.

Table 4: ^{119}Sn Mössbauer parameters for the tin catalysts at room temperature

Sample	Stage[a]	δ (mm.s^{-1})[b,c]	Δ (mm.s^{-1})[c]	n[d]	Contr. (%)[e]	Assignment[f]
MB-586	nc	-0.09	0.15	+4	95	Sn/O octa. dist.
MB-586	nc	3.04	1.59	+2	5	SnO_3E or SnO_4E
MB-586	c	-0.03	0.30	+4	100	Sn/O octa. dist.
MB-586	u	-0.03	0.40	+4	99	Sn/O octa. dist.
MB-586	u	3.16	0.98	+2	1	SnS
MB-599	nc	-0.09	0.40	+4	75	Sn/O octa. dist.
MB-599	nc	3.13	1.78	+2	25	SnO_3E or SnO_4E
MB-599	c	-0.03	0.10	+4	100	Sn/O octa. Dist.
MB-599	u(63)	-0.03	0.10	+4	85	Sn/O octa. dist.
MB-599	u(63)	3.22	0.86	+2	15	SnS
MB-599	u(76)	-0.03	0.10	+4	90	Sn/O octa. dist.
MB-599	u(76)	3.28	0.86	+2	10	SnS

Notes:

a) Stage nc = non-calcined, c = calcined, u = used, runs 63 and 76: as in Table 3.
b) δ = isomer shift relative to $CaSnO_3$ at room temperature.
c) δ and Δ : error bar = 0.01.
d) n = tin oxidation state.
e) contr.(%): % contribution to the total spectrum; error bar = 1%.
f) Sn/O octa. dist.: distorted octahedral environment of oxygen;
SnO_3E and SnO_4E: see text.

Table 5: Petrographic analysis of THF insoluble residues (in vol % mineral matter free)

Catalyst	Unaltered coal	Altered huminite	Granular residues	Semicoke[a]	Coal/pitch-derived solids[b]
Sn	0.2	29.5	0.0	51.4	18.8
Zn	1.2	63.9	0.0	25.2	9.6
Blank	0.4	52.8	0.4	33.4	12.9
Ni	2.2	83.6	14.1	0.0	0.0
Co-Mo	3.5	80.5	16.1	0.0	0.0
Pd	3.2	80.7	16.1	0.0	0.0
Mo	2.6	82.5	14.9	0.0	0.0
MB-531	1.6	95.5	2.9	0.0	0.0

Notes:
a) Anisotropic
b) Isotropic

FIGURE CAPTIONS

Figure 1: SEM micrograph of sodium hydrous titanate before cationic exchange (top: 5,000 x magnification; bottom: 10,000 x mag.).

Figure 2: SEM micrograph of calcined tin hydrous titanate, MB-599 (top: 1,000 x mag.; bottom: 10,000 x mag.).

Figure 3: Incremental pore volume as a function of pore diameter, (from mercury porosimetry data) for Co-Mo catalysts supported on alumina (MB-531) or on hydrous titanate.

Figure 4: X-ray powder pattern of the MB-586 catalyst at various stages: (a)= support, (b)= non-calcined ion-exchanged catalyst, (c)= calcined catalyst, (d)= used catalyst in THF insolubles. The peaks labelled X on pattern (b) could not be identified. The peak labelled X on patterns (c) and (d) is assigned to (101) $Ti_{1-x}Sn_xO_2$ rutile solid solution (see Fig. 5). The interpolated baseline (dashed line) is just a guide for the eye.

Figure 5: X-ray powder pattern of the MB-599 catalyst at various stages: (a)= support, (b)= non-calcined ion-exchanged catalyst, (c)= calcined catalyst, (d)= used catalyst in THF insolubles of run 63, (e)= used catalyst in THF insolubles of run 76. The interpolated baseline (dashed line) is just a guide for the eye.

Figure 6: Yields of oil, asphaltenes, preasphaltenes and THF insolubles for MEHT catalysts tested at 410°C (O = oil, W = aqueous phase, A = asphaltenes, P = preasphaltenes, T = THF insolubles, R = gas and loss).

Figure 7: Yields of oil, asphaltenes, preasphaltenes and THF insolubles for Co-Mo catalysts supported on alumina (MB-531) or on hydrous titanate, and tested at 410 and 430°C (Letters defined in Fig. 6).

Figure 8: Yields of gases including losses for MEHT catalysts tested at 410°C.

Figure 9: Performance of MEHT catalysts for hydrodesulphurization.

Fig. 1

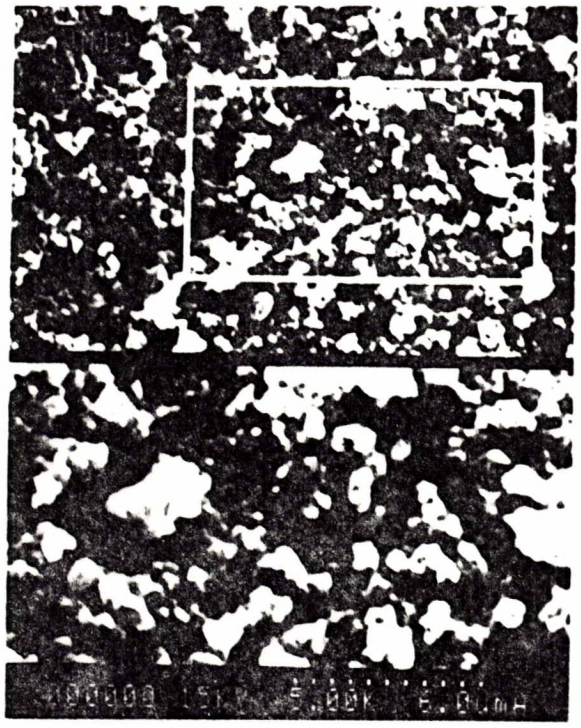

Fig. 2

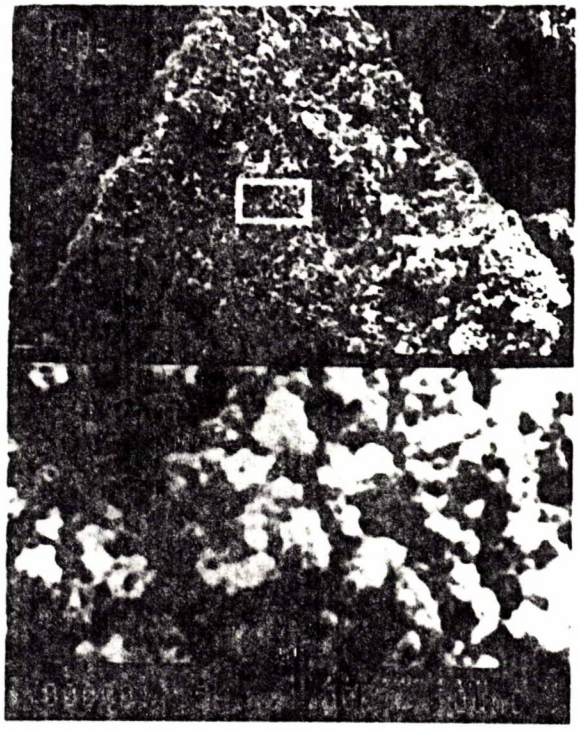

Fig. 3

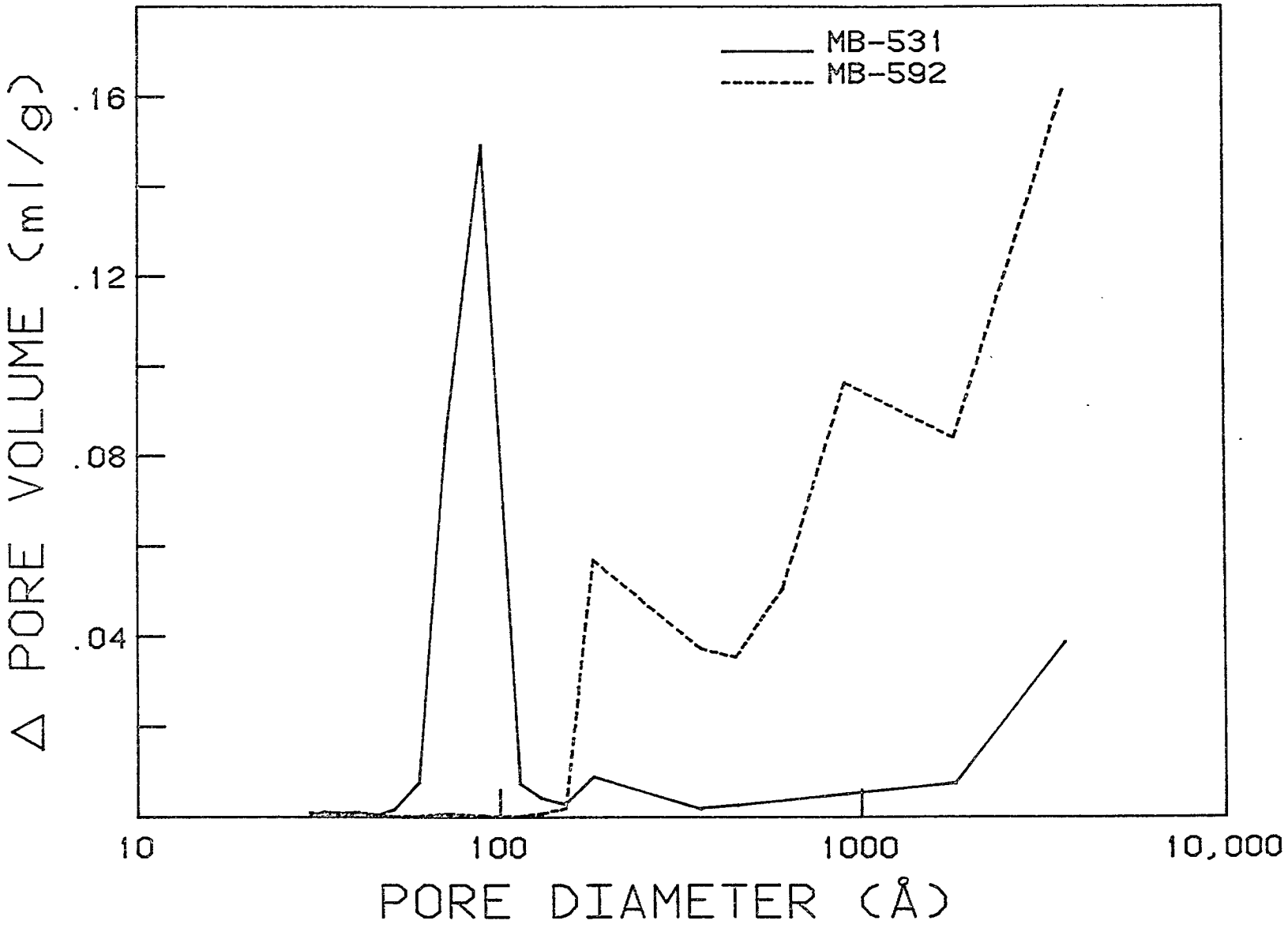
MB-531
MB-592
Δ PORE VOLUME (ml/g)
.16
.12
.08
.04
10
100
1000
10,000
PORE DIAMETER (Å)

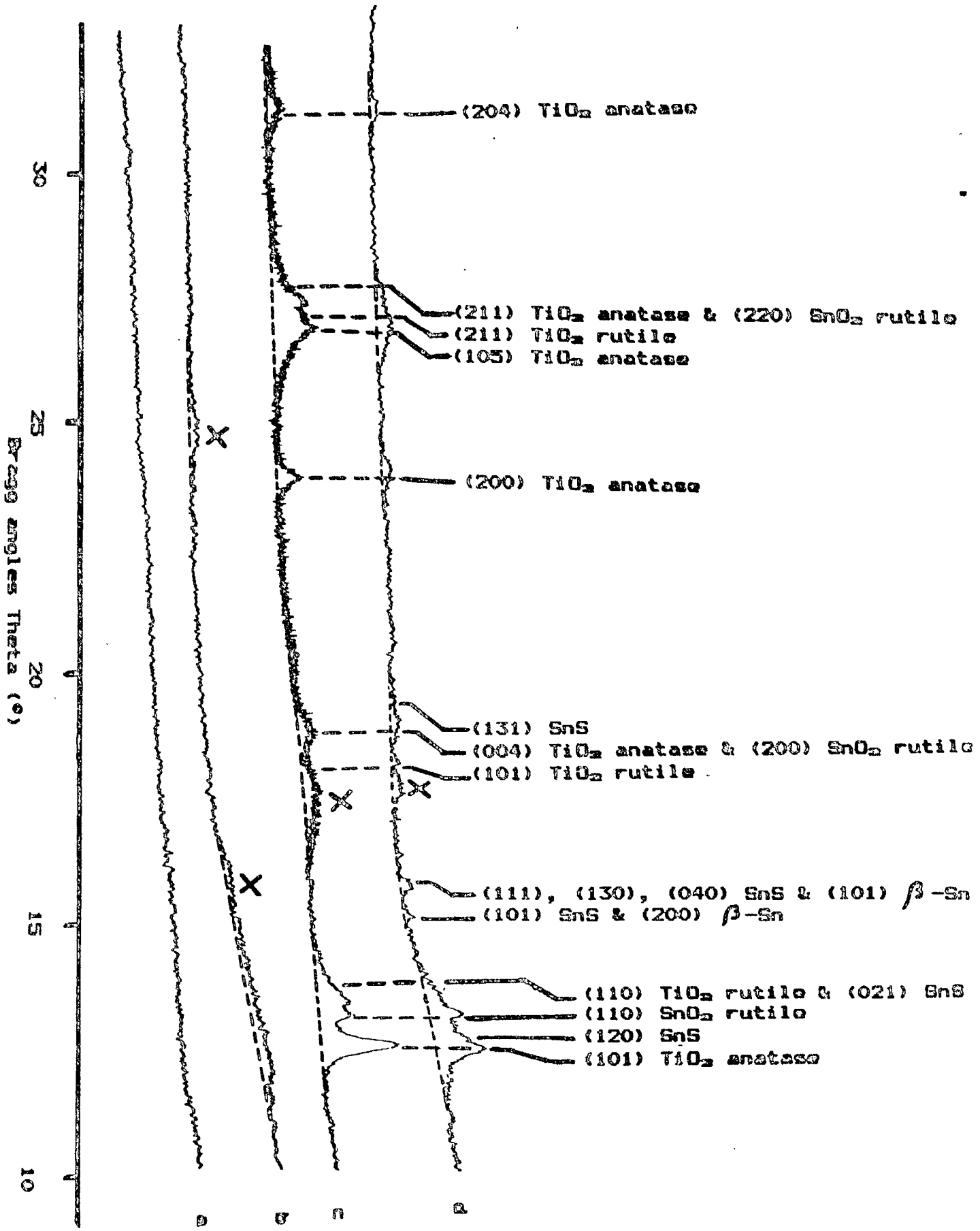
(204) TiO2 anatase
(211) TiO2 anatase & (220) SnO2 rutile
(211) TiO2 rutile
(105) TiO2 anatase
(200) TiO2 anatase
(131) SnS
(004) TiO2 anatase & (200) SnO2 rutile
(101) TiO2 rutile
(111), (130), (040) SnS & (101) β-Sn
(101) SnS & (200) β-Sn
(110) TiO2 rutile & (021) SnS
(110) SnO2 rutile
(120) SnS
(101) TiO2 anatase
10
15
20
25
30
2θ (deg) angles Theta (°)

Fig. 4

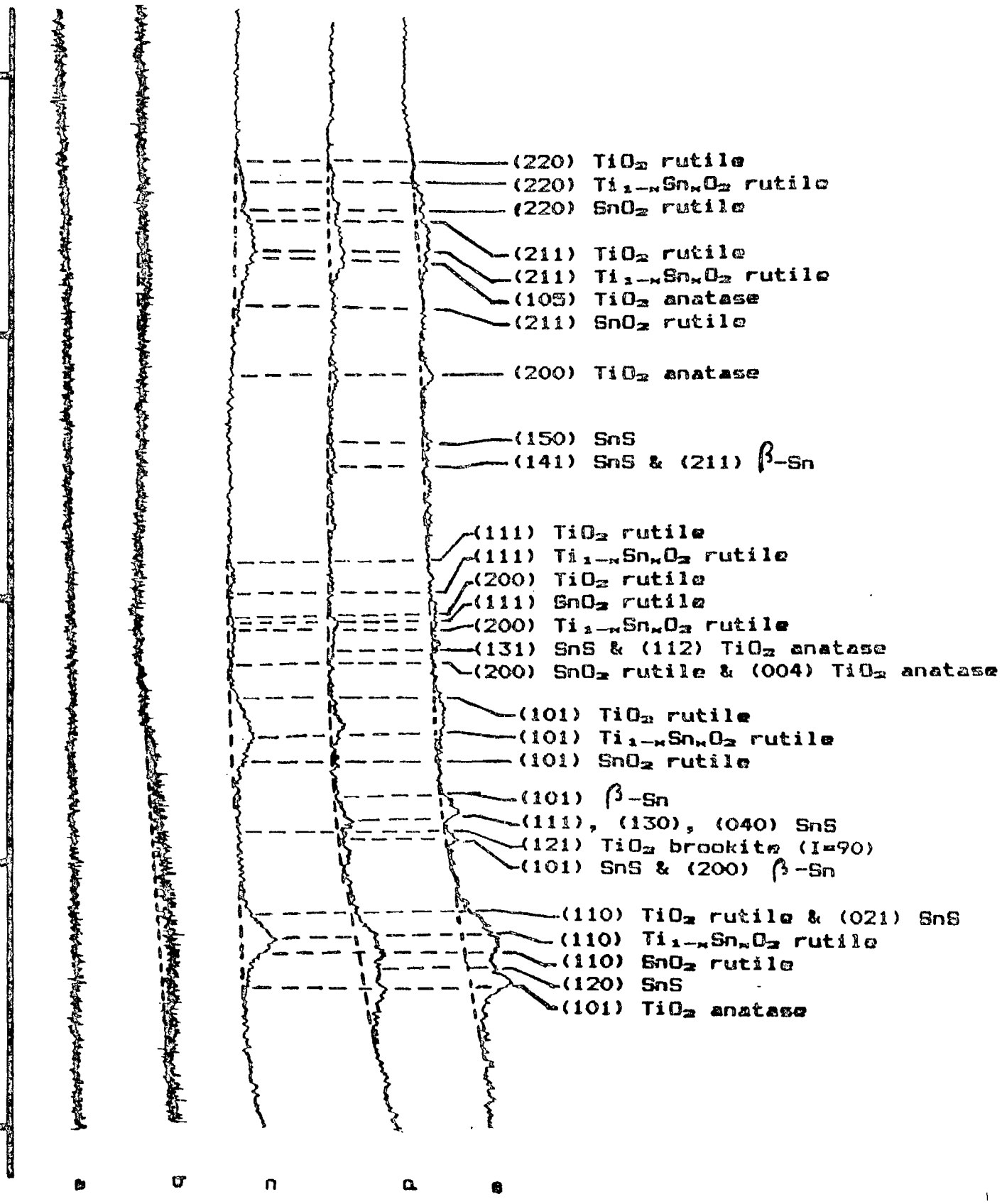
(220) TiO2 rutile
(220) Ti1-xSnxO2 rutile
(220) SnO2 rutile
(211) TiO2 rutile
(211) Ti1-xSnxO2 rutile
(105) TiO2 anatase
(211) SnO2 rutile
(200) TiO2 anatase
(150) SnS
(141) SnS & (211) β-Sn
(111) TiO2 rutile
(111) Ti1-xSnxO2 rutile
(200) TiO2 rutile
(111) SnO2 rutile
(200) Ti1-xSnxO2 rutile
(131) SnS & (112) TiO2 anatase
(200) SnO2 rutile & (004) TiO2 anatase
(101) TiO2 rutile
(101) Ti1-xSnxO2 rutile
(101) SnO2 rutile
(101) β-Sn
(111), (130), (040) SnS
(121) TiO2 brookite (I=90)
(101) SnS & (200) β-Sn
(110) TiO2 rutile & (021) SnS
(110) Ti1-xSnxO2 rutile
(110) SnO2 rutile
(120) SnS
(101) TiO2 anatase
30
25
20
15
10
Bragg angles Theta (o)

Fig. 6

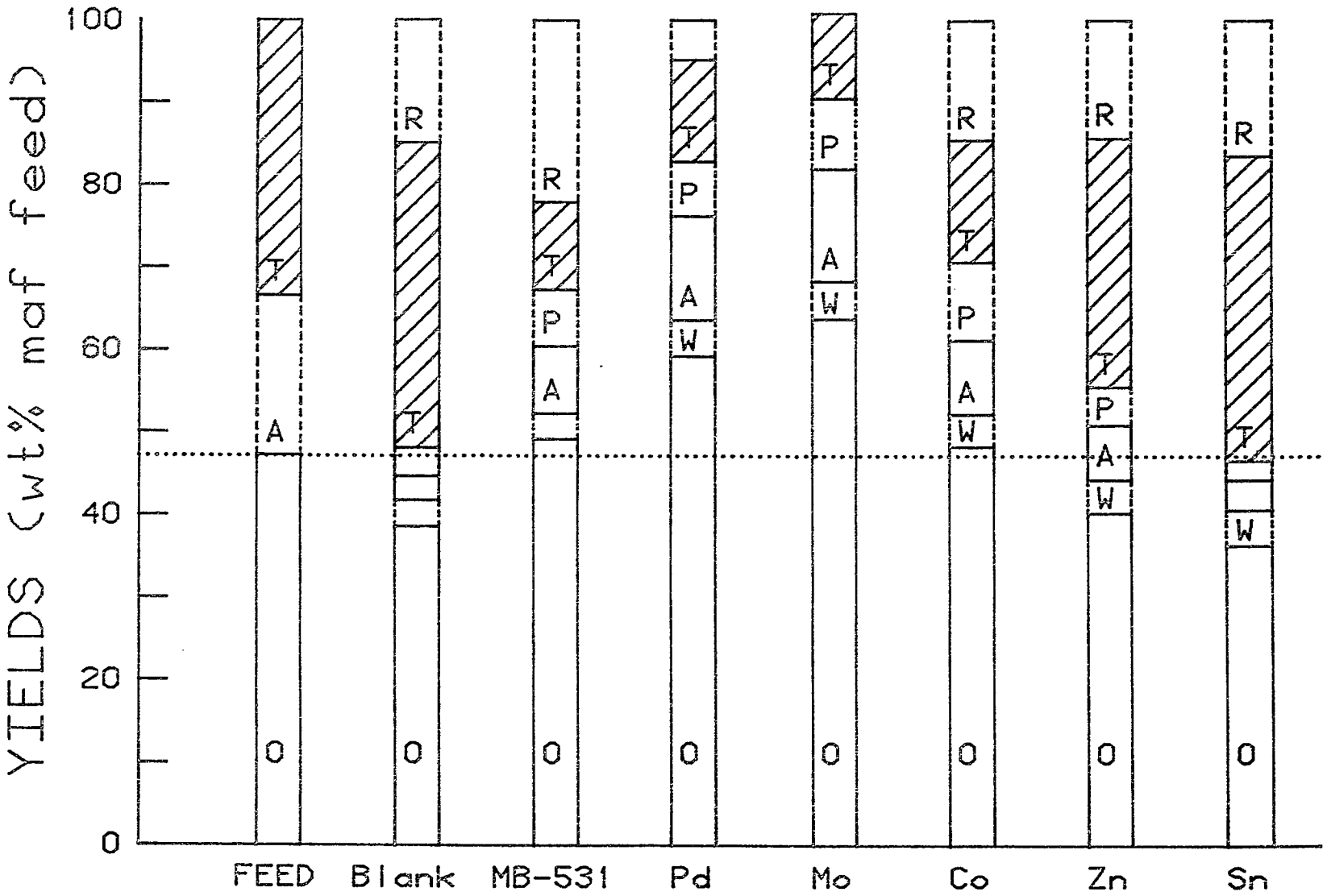
YIELDS (wt% maf feed)
100
80
60
40
20
0
R
T
P
A
W
O
FEED
Blank
MB-531
Pd
Mo
Co
Zn
Sn

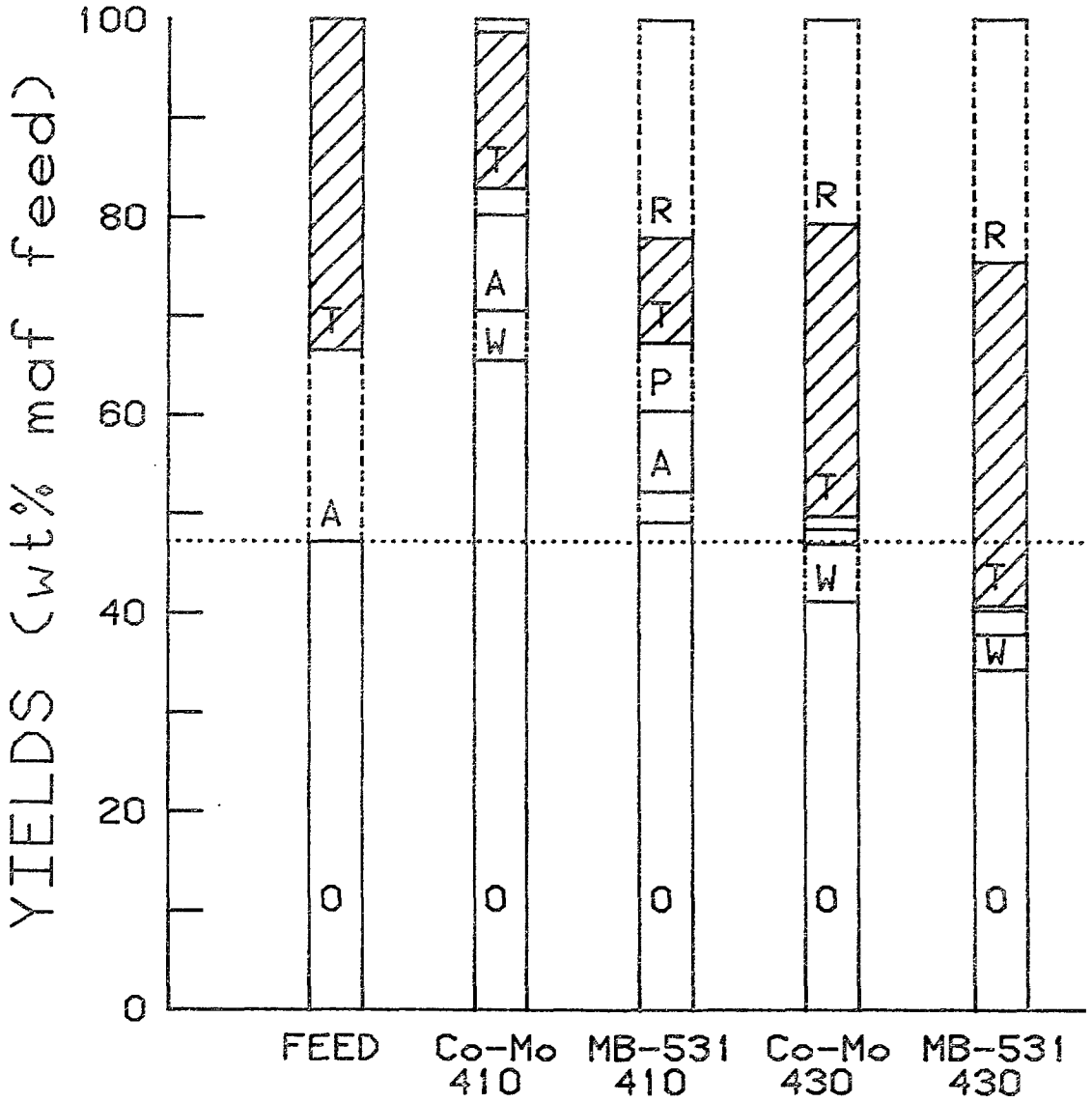
YIELDS (wt% maf feed)
100
80
60
40
20
0
A
T
O
T
A
W
O
R
T
P
A
O
R
T
W
O
R
T
W
O
FEED
Co-Mo 410
MB-531 410
Co-Mo 430
MB-531 430

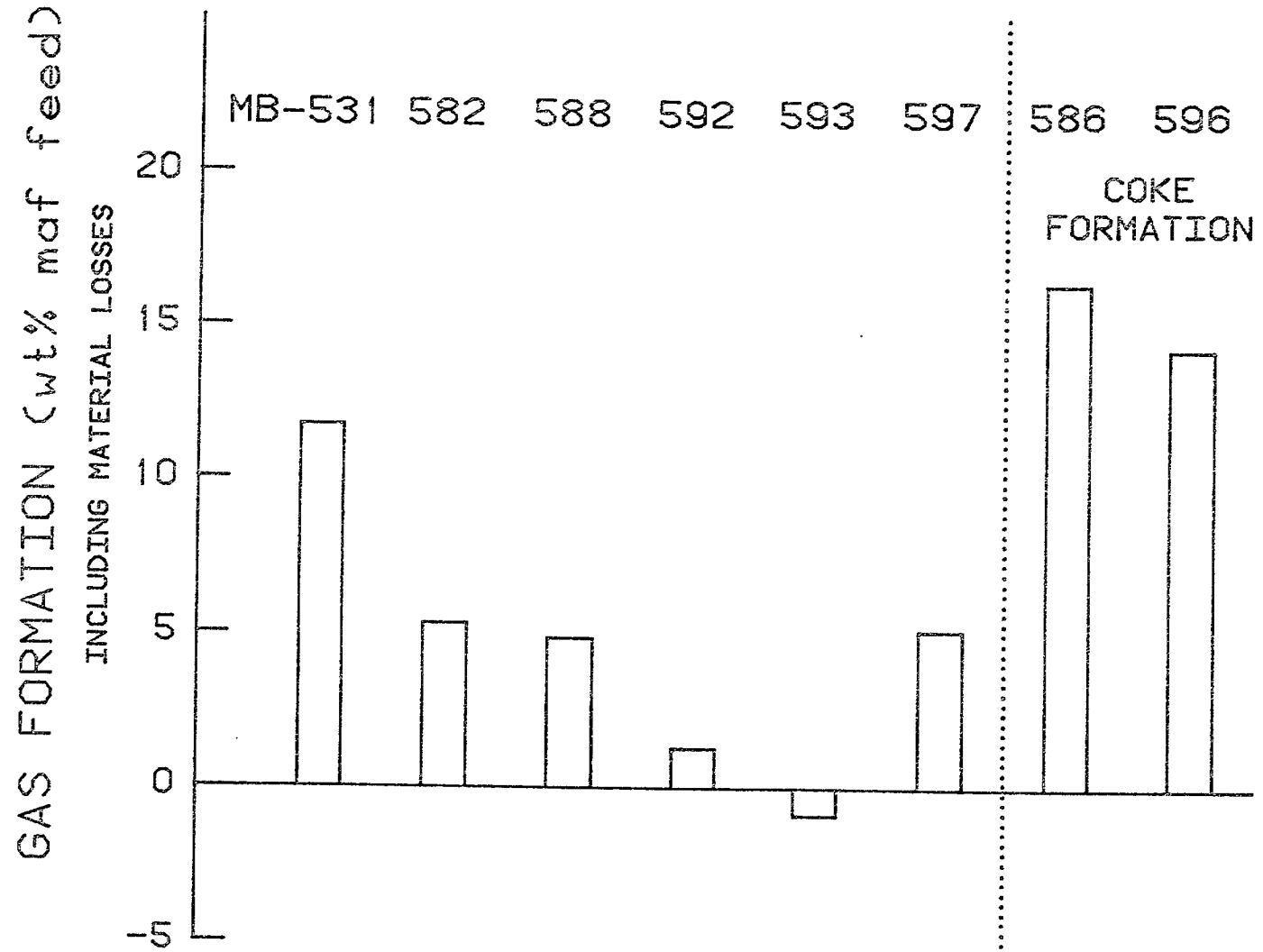
GAS FORMATION (wt% maf feed)
INCLUDING MATERIAL LOSSES
20
15
10
5
0
-5
MB-531
582
588
592
593
597
586
596
COKE FORMATION

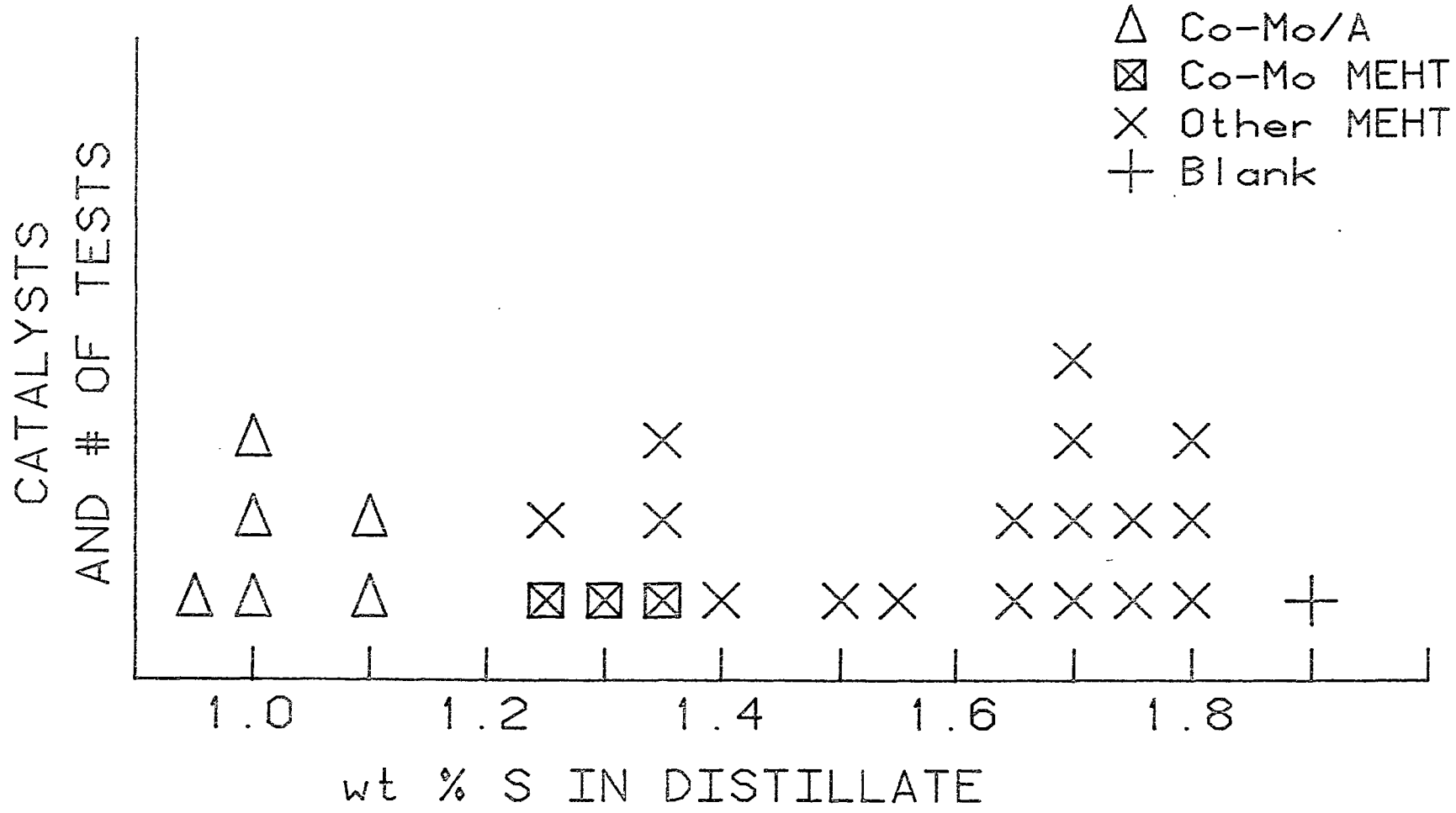
Δ Co-Mo/A
⊠ Co-Mo MEHT
X Other MEHT
+ Blank
CATALYSTS
AND # OF TESTS
1.0
1.2
1.4
1.6
1.8
wt % S IN DISTILLATE